

# Enhanced resistance of DNA nanostructures to enzymatic digestion†

Jung-Won Keum<sup>a</sup> and Harry Bermudez<sup>\*b</sup>

Received (in Austin, TX, USA) 27th August 2009, Accepted 23rd September 2009

First published as an Advance Article on the web 13th October 2009

DOI: 10.1039/b917661f

**The ability of nucleases to perform their catalytic functions depends on the sequence and structural features of target DNA substrates. Due to their size and shape, several DNA tetrahedra are resistant to the action of specific and non-specific nucleases. Such enhanced stability is a key requirement for DNA nanostructures to be useful as delivery vehicles.**

DNA nanotechnology is increasingly used to create well-defined functional structures.<sup>1,2</sup> Numerous 2-D and 3-D objects have been built entirely from DNA,<sup>3–6</sup> in addition to proof-of-concept devices.<sup>7–9</sup> While DNA structures have potential as vehicles for gene and drug delivery,<sup>10–12</sup> the ability to avoid rapid degradation *in vivo* is needed. For discrete DNA nanostructures with dimensions much smaller than 50 nm, enzymatic recognition might be quite different from that of linear DNA. Indeed, here we report the enhanced stability of various DNA tetrahedra with respect to degradation by various enzymes.

We began by comparing digestion patterns between DNA tetrahedra and linear DNA structures. Following the design of Goodman *et al.*,<sup>13</sup> we assembled a tetrahedron (T1) having edges of 20 bp in length, or about 7 nm, containing a single centrally-located DdeI restriction site (Fig. 1). DdeI is a type II restriction enzyme<sup>14</sup> that specifically recognizes and cleaves within the sequence CTNAG. To examine the effect of site placement within the pyramid, we designed a variant of the above 20 bp tetrahedron having its DdeI site located adjacent to a vertex (T2), with the overall sequence identical to T1. As controls we also assembled corresponding “linear” structures containing restriction sites identical to regions in T1 and T2. One type of linear structure (L1 and L2) has a central complementary region of 20 bp, with the remainder unhybridized. Another type of linear structure (L3) is made of two perfectly complementary strands. Assembly of both T1 and T2 were confirmed by using native polyacrylamide gel electrophoresis (Fig. S1†).<sup>15</sup>

Digestion with DdeI is easily performed, because generation of the recognition site occurs naturally during self-assembly of the tetrahedron, and therefore does not require ligation. While DdeI cleaves T1 as easily as L1 and L3, consistent with the findings of Goodman,<sup>13</sup> we hypothesized that location of restriction sites might affect the ability to be digested. In

contrast to T1, T2 has its DdeI site located immediately adjacent to a vertex. Subsequent incubation of unligated T1 and T2 with DdeI showed no difference when compared to linear controls (Fig. S2†), suggesting that the DdeI can access the site or distort unligated tetrahedra sufficiently to be active.

The increased mechanical stability of a ligated DNA nanostructure would presumably be more resistant to enzymatic attack. We therefore ligated the nicks in T1 and T2 to form covalent circular strands, and subsequently incubated with exonuclease III (Exo III) to remove any unligated strands and free ends. Exo III primarily recognizes 3'-hydroxyls that are recessed or blunt, and digests towards the 5'-end,<sup>16,17</sup> leaving only circular DNA forms intact. Following Exo III inactivation and re-assembly, digestion with DdeI was analyzed by denaturing PAGE (Fig. 2). Because of the ligation and Exo III treatment, any DdeI cleavage leads to the appearance of linear DNA fragments. While DdeI degrades ligated T1 to yield multiple linear fragments, there are no such species for ligated T2, suggesting near-complete protection from cleavage. The linear forms L1 (Fig. S2†), L2, and L3 are readily digested by DdeI, indicating that protection is due to the combination of site location and a covalently closed nanostructure.

We next examined the resistance to non-specific enzymatic degradation, where the role of sequence composition is expected to be minimal. Fig. 3 shows the digestion products upon incubation with DNase I,<sup>17</sup> an endonuclease that non-specifically cleaves DNA to produce fragments of varying lengths. Unligated T1 is gradually digested by DNase I, but

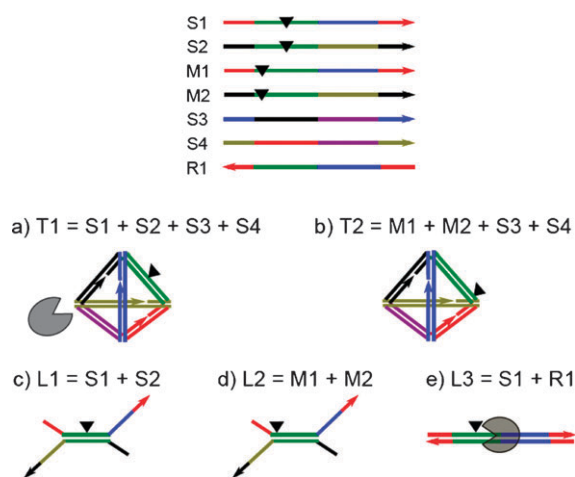


**Fig. 1** Schematic of DNA strands and self-assembled structures. Various DNA substrates are listed from (a) to (e). In T1 and T2, two edges (green and purple) are free from “nicks” following hybridization. Sections of L1–L3 are identical in sequence to sections of T1 and T2. The DdeI endonuclease cleavage site is indicated by the black triangles. Sequences of the DNA strands are given in the ESI†.

<sup>a</sup> Department of Chemical Engineering, University of Massachusetts, Amherst, MA, USA

<sup>b</sup> Department of Polymer Science and Engineering, University of Massachusetts, Amherst, MA, USA.

E-mail: bermudez@polysci.umass.edu; Fax: +1 413 545 0082;

Tel: +1 413 577 1413

† Electronic supplementary information (ESI) available: DNA sequences, assembly conditions, details of digestion and analysis. See DOI: 10.1039/b917661f

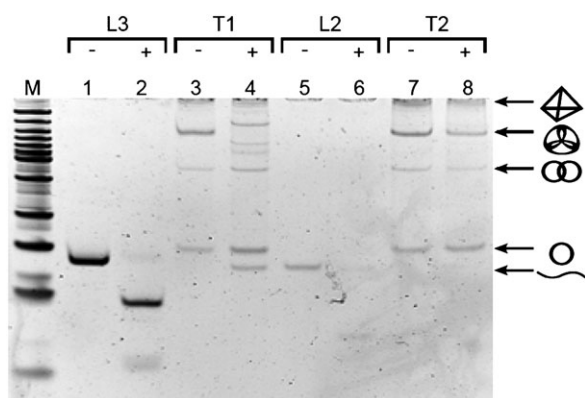


**Fig. 2** Denaturing PAGE of ligated tetrahedra T1 and T2 and their corresponding “linear” analogues (L3 and L2) digested with DdeI endonuclease. The “-” and “+” denote the absence or presence of DdeI, respectively. The symbols to the right of the gel indicate various covalent circular forms resulting from ligation and a linear fragment resulting from cleavage. DdeI degrades all linear forms and T1, but not T2, as inferred from the absence of linear digestion products.

more slowly than L3. Analyzing the band intensities shows that T1 has a decay time constant nearly three times greater than L3 (Fig. 3c). Under physiological levels of DNase I, such time constants would be correspondingly larger. Our experiments were performed at  $10 \text{ U mL}^{-1} = 7 \mu\text{g mL}^{-1}$ ; a large excess when compared to reported serum levels of  $0.36 \text{ U mL}^{-1}$ ,<sup>18</sup> and  $13 \text{ ng mL}^{-1}$ .<sup>19</sup> The differences in digestion can be attributed to the known sensitivity of DNase I activity to both local and global helix geometry,<sup>17,20</sup> which are likely to differ between tetrahedral and linear structures. In addition, while the degradation products of both L1 and L3 are polydisperse (as expected), the digestion products of T1 appear to be largely a specific fragment. Because each vertex of the tetrahedron has the same topology as a 3-way branch junction, we presume that sites near vertices are protected from DNase I digestion, as has been shown for planar 3- and 4-way branches.<sup>21</sup> Such protection near vertices, consistent with the results of Fig. 2, implies that cleavage is occurring closer to the mid-points of the edges, preferentially producing a specific fragment size.

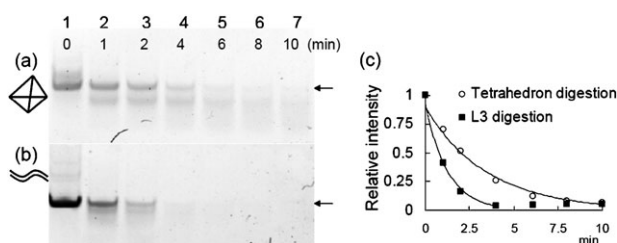


**Fig. 3** Denaturing PAGE of products from non-specific digestion by 0.2 units of DNase I, with arrows denoting uncut DNA. (a) Digestion of the unligated tetrahedron T1 is gradual and appears to generate a well-defined product, consistent with the activity of DNase I near “branch” junctions. (b) Digestion of “linear” DNA L3 is rapid and truly non-specific, generating a distribution of fragment sizes (which cannot be visualized on the gel). Individual lanes are marked with the incubation time in minutes. (c) Band intensities are well-described by first-order decay, yielding corresponding time constants.

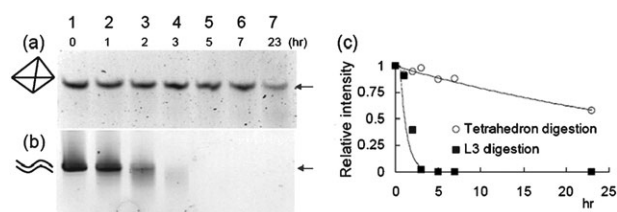


**Fig. 4** Denaturing PAGE of products from non-specific digestion by 10% FBS, with arrows denoting uncut DNA. (a) The unligated tetrahedron T1 is significantly more stable than its (b) “linear” counterpart L3. Individual lanes are marked with the incubation time in hours. (c) Band intensities are well-described by first-order decay, yielding corresponding time constants.

Towards more closely mimicking physiological conditions, we incubated unligated T1 and its linear counterparts in the presence of 10% fetal bovine serum. In this complex mixture of nucleases and other proteins, T1 is significantly more stable than either L1 or L3 (Fig. 4). From fits of the data to first-order kinetics (Fig. 4c), the decay time constants differ by nearly a factor of fifty: 0.8 h for L3 and 42 h for T1. This striking stability in serum was unexpected, because serum contains a mixture of both endo- and exo-nucleases, and thus an unligated tetrahedron is susceptible to two modes of degradation. Interestingly, recent reports of circular DNA aptamers also indicate that small and discrete DNA objects are resistant to serum degradation,<sup>22</sup> thought to be primarily by the lack of 3' ends. Therefore, the results of Fig. 2 suggest that the ligation of nicks provides dual protection: elimination of 3' ends *and* an increased rigidity of the tetrahedron.

Determining the actual mechanism underlying the enhanced resistance of tetrahedra to enzymatic attack requires further study, but the results point to several possibilities. Depending on the enzyme, recognition can be based upon DNA sequence, backbone geometry, groove width, curvature and flexibility.<sup>17</sup> Consider the role of enzyme binding: it is well known that restriction endonucleases initially bind non-specifically and with low affinity, followed by diffusion along the DNA.<sup>23,24</sup> However, the equilibrium binding constant is independent of length.<sup>25</sup> Comparing the various digestions of T1 against either L1 or L3 suggests that steric hindrance introduced by the nanostructure may reduce the effective binding of enzymes to DNA. Whether through size or geometry, such a steric barrier would inhibit cleavage, regardless of whether the enzyme acts specifically or non-specifically.

Furthermore, crystal structures of bacterial restriction endonucleases bound to DNA appear to distort the DNA helix upon reaching their recognition sites.<sup>14</sup> There is also evidence for the non-specific cleavage by mammalian DNase I being determined by bending distortions.<sup>26,27</sup> Such mechanically strained DNA–enzyme complexes are thought to be the transition-state intermediates required for hydrolysis. Therefore the ability of both DNA and nucleases to undergo conformational changes is essential for cleavage. Noting that dsDNA is generally viewed as stiff below its persistence length  $p = 50 \text{ nm}$ ,<sup>28</sup> a given arc length distortion requires more force to bend for shorter DNA strands. From the length of hybridized DNA, L1 might be expected to be as flexible as any edge of T1, but a tetrahedron has additional rigidity imparted

by the connectivity of the 3-D structure, where distortions to one edge will be collectively opposed by the remaining five edges. Such a rigidity effect would be further enhanced by ligation of nicks, as implied by Fig. 2.

In summary, the unusual stability of a DNA tetrahedron to enzymatic degradation is a result of a combined inhibition of both binding and catalytic activity. If a smaller tetrahedron could be constructed, it might be still further protected against enzymatic degradation. Other types of branched geometries, or curvatures, may also be a means of protection.<sup>29</sup> Such an approach contrasts with the use of chemically modified nucleic acids to minimize degradation,<sup>30</sup> which can introduce toxicity as well as triggering unwanted immune responses. When the goal is to modulate gene expression through antisense or siRNA mechanisms, synthetic analogues might not be recognized by RNaseH or RISC.<sup>31</sup> By contrast, antisense and siRNA sequences can be directly incorporated into DNA nanostructures, making these objects both vehicle and therapeutic. Incorporation of cell-targeting capability is possible by using aptamer sequences, with RNaseH or RISC activity triggered through hybridization of complementary sequences to generate target structures. If release from the nanostructure is needed, partially hybridized regions can facilitate strand “extraction”.

Finally, optimization of DNA structures in regard to digestion resistance seems possible with *in vitro* evolutionary techniques such as SELEX (systematic evolution of ligands by exponential enrichment).<sup>32</sup> The demonstration here of improved stability in challenging environments strengthens the possibility of using DNA nanostructures as drug or gene delivery vehicles, with the incorporation of cell-recognition and responsive features remaining an open challenge.

The authors thank C. Woodcock for initial discussions, Lorenzo Ramos-Mucci for technical assistance, and the NSF (CMMI-0531171) for financial support.

## Notes and references

- 1 F. A. Aldaye, A. L. Palmer and H. F. Sleiman, *Science*, 2008, **321**, 1795–1799.
- 2 U. Feldkamp and C. M. Niemeyer, *Angew. Chem., Int. Ed.*, 2008, **47**, 3871–3873.
- 3 E. S. Andersen, M. Dong, M. M. Nielsen, K. Jahn, R. Subramani, W. Mamdouh, M. M. Golas, B. Sander, H. Stark, C. L. P. Oliveira, J. S. Pedersen, V. Birkedal, F. Besenbacher, K. V. Gothelf and J. Kjems, *Nature*, 2009, **459**, 73–76.
- 4 J. H. Chen and N. C. Seeman, *Nature*, 1991, **350**, 631–633.
- 5 D. Liu, S. H. Park, J. H. Reif and T. H. LaBean, *Proc. Natl. Acad. Sci. U. S. A.*, 2004, **101**, 717–722.
- 6 P. W. K. Rothemund, *Nature*, 2006, **440**, 297–302.
- 7 R. D. Barish, P. W. K. Rothemund and E. Winfree, *Nano Lett.*, 2005, **5**, 2586–2592.
- 8 R. P. Goodman, M. Heilemann, S. Dooset, C. M. Erben, A. N. Kapanidis and A. J. Turberfield, *Nat. Nanotechnol.*, 2008, **3**, 93–96.
- 9 Y. Ke, J. Nangreave, H. Yan, S. Lindsay and Y. Liu, *Chem. Commun.*, 2008, 5622–5624.
- 10 B. P. Duckworth, Y. Chen, J. W. Wollack, Y. Sham, J. D. Mueller, T. A. Taton and M. D. Distefano, *Angew. Chem., Int. Ed.*, 2007, **46**, 8819–8822.
- 11 C. M. Erben, R. P. Goodman and A. J. Turberfield, *Angew. Chem., Int. Ed.*, 2006, **45**, 7414–7417.
- 12 S. Ko, H. Liu, Y. Chen and C. Mao, *Biomacromolecules*, 2008, **9**, 3039–3043.
- 13 R. P. Goodman, I. A. T. Schaap, C. F. Tardin, C. M. Erben, R. M. Berry, C. F. Schmidt and A. J. Turberfield, *Science*, 2005, **310**, 1661–1665.
- 14 A. Pingoud and A. Jeltsch, *Nucleic Acids Res.*, 2001, **29**, 3705–3727.
- 15 R. P. Goodman, R. M. Berry and A. J. Turberfield, *Chem. Commun.*, 2004, 1372–1373.
- 16 C. C. Richardson, I. R. Lehman and A. Kornberg, *J. Biol. Chem.*, 1964, **239**, 251–258.
- 17 D. Suck, *Biopolymers*, 1997, **44**, 405–421.
- 18 A. Cherepanova, S. Tamkovich, D. Pysnyi, M. Kharkova, V. Vlassov and P. Laktionov, *J. Immunol. Methods*, 2007, **325**, 96–103.
- 19 E. Tinazzi, A. Puccetti, R. Gerli, A. Rigo, P. Migliorini, S. Simeoni, R. Beri, M. Dolcino, N. Martinelli, R. Corrocher and C. Lunardi, *Int. Immunol.*, 2009, **21**, 237–243.
- 20 H. R. Drew and A. A. Travers, *Cell*, 1984, **37**, 491–502.
- 21 M. Lu, Q. Guo, N. C. Seeman and N. R. Kallenbach, *J. Biol. Chem.*, 1989, **264**, 20851–20854.
- 22 D. A. Di Giusto and G. C. King, *J. Biol. Chem.*, 2004, **279**, 46483–46489.
- 23 H. J. Ehbrecht, A. Pingoud, C. Urbanke, G. Maass and C. Gualerzi, *J. Biol. Chem.*, 1985, **260**, 6160–6166.
- 24 S. E. Halford and J. F. Marko, *Nucleic Acids Res.*, 2004, **32**, 3040–3052.
- 25 W. E. Jack, B. J. Terry and P. Modrich, *Proc. Natl. Acad. Sci. U. S. A.*, 1982, **79**, 4010–4014.
- 26 I. Brukner, R. Sanchez, D. Suck and S. Pongor, *EMBO J.*, 1995, **14**, 1812–1818.
- 27 M. E. Hogan, M. W. Roberson and R. H. Austin, *Proc. Natl. Acad. Sci. U. S. A.*, 1989, **86**, 9273–9277.
- 28 R. S. Mathew-Fenn, R. Das and P. A. B. Harbury, *Science*, 2008, **322**, 446–449.
- 29 Y. He, T. Ye, M. Su, C. Zhang, A. E. Ribbe, W. Jiang and C. Mao, *Nature*, 2008, **452**, 198–201.
- 30 M. A. Behlke, *Oligonucleotides*, 2008, **18**, 305–319.
- 31 T. V. Achenbach, B. Brunner and K. Heermeier, *ChemBioChem*, 2003, **4**, 928–935.
- 32 D. S. Wilson and J. W. Szostak, *Annu. Rev. Biochem.*, 1999, **68**, 611–647.